

# Relationship Between Secondary Twins and Pyramidal Dislocations in a Mg-3Al-1Zn Alloy During High Cycle Fatigue Deformation

Tan Li, Zhang Xiyan, Xia Ting, Huang Guangjie, Liu Qing

Chongqing University, Chongqing 400044, China

**Abstract:** Typical fracture morphology of Mg-3Al-1Zn alloy after cyclic deformation was investigated using optical microscope (OM), scanning electron microscopy (SEM), transmission Kikuchi diffraction (TKD) and transmission electron microscopy (TEM). Cross-section samples were extracted from secondary twin regions for TEM/TKD observation. The results show that a large amount of  $\{10\bar{1}2\}$ - $\{10\bar{1}2\}$  secondary twins are observed in the region near the fractured edge. Two-beam bright field (TBBF) technique was applied to study the types of dislocations along secondary twin boundaries. It is found that pyramidal dislocations are highly active within  $\{10\bar{1}2\}$ - $\{10\bar{1}2\}$  secondary twins, which is considered to be related to  $\{10\bar{1}2\}$ - $\{10\bar{1}2\}$  secondary twins. Localized stress concentration within the secondary twins may lead to the formation of pyramidal dislocations.

**Key words:** secondary twins; pyramidal dislocations; magnesium; fatigue

Fatigue is the cumulative damage of materials caused by cyclic loading, often resulting in fracture and catastrophic failure of components<sup>[1]</sup>. There have been numerous reports on the fatigue behavior of magnesium alloys. A major focus is on the role of tensile twinning in fatigue deformation and failure mechanisms<sup>[2-5]</sup>. However, Koike et al.<sup>[6-8]</sup> reported that besides twinning, dislocation slip is another important deformation mechanism during cyclic deformation in Mg alloys.

Combined with plenty of previous research results<sup>[9, 10]</sup>, there are three different types of dislocations in hcp metals. Basal  $\langle a \rangle$  is the easiest slip mode due to its lowest CRSS (critical resolved shear stress)<sup>[10, 11]</sup>, while pyramidal  $\langle c + a \rangle$  is the most difficult slip mode, but yet necessary, pyramidal slip mode was reported to accommodate the plastic strains along  $c$ -axis<sup>[12-14]</sup>. Xie et al.<sup>[12]</sup> observed pyramidal slip traces on a single Mg crystal surface when compressed along  $c$ -axis at room temperature. Obara et al.<sup>[13]</sup> performed TEM on Mg single crystal, and  $\langle c + a \rangle$  dislocations were observed when the samples were subjected to  $c$ -axis compression tests. Syed et al.<sup>[14]</sup> confirms  $\langle c + a \rangle$  were present

when compressed along the [0001] direction in a single-crystal Mg. These results has pointed to the importance of  $\langle c + a \rangle$  dislocation slip. More recently, we have found large amount of pyramidal dislocations existed in fatigued samples at high stress amplitude<sup>[15]</sup>. The general consensus points out that high stress concentration may result in activation of pyramidal dislocations. There are several reasons for stress concentration during the deformation process in hcp metals. For instance, it is possible that the dislocations pile ups would lead to stressing concentration along grain or twin boundaries during the loading-unloading deformation process<sup>[16]</sup>. Agnew et al.<sup>[9]</sup> postulated that  $\langle c + a \rangle$  dislocations were generated at the tip of mechanical twins, producing high stress concentration. And Xin et al.<sup>[17]</sup> reported that the interaction of different twin variants may induce stress concentration. In addition, Lentz et al.<sup>[18]</sup> reported  $\langle c + a \rangle$  dislocations has a relationship with  $\{10\bar{1}1\}$ - $\{10\bar{1}2\}$  double twins. In another recent paper<sup>[19]</sup>,  $\{10\bar{1}2\}$ - $\{10\bar{1}2\}$  twinning mode was found to be a secondary twinning mode in magnesium alloys during cyclic de-

Received date: June 25, 2018

Foundation item: National Natural Science Foundation of China (51671040, 50890170, 51421001); National Basic Research Program of China (2010CB631004)

Corresponding author: Zhang Xiyan, Ph. D., Professor, College of Materials Science and Engineering, Chongqing University, Chongqing 400044, P. R. China, E-mail: kehen888@163.com

Copyright © 2019, Northwest Institute for Nonferrous Metal Research. Published by Science Press. All rights reserved.

formation<sup>[19]</sup>, but with no direct evidence of the relationship between pyramidal dislocations and secondary twins. Therefore, the reason of activation of pyramidal is needed to clarify in Mg and its alloys under cyclic deformation.

In the current study, we present the result of a transmission Kikuchi diffraction (TKD) study of hot-rolled AZ31 Mg alloy by cyclic deformation. The aim of this research is to identify which kind of dislocation patterns are presented along secondary twins boundaries during cyclic deformation at room temperature and to clarify the relationship between pyramidal dislocations and secondary twins.

## 1 Experiment

The fatigue tests of the present work are described in the previous report<sup>[15]</sup>.  $\{10\bar{1}2\}-\{10\bar{1}2\}$  secondary twins were identified at 90 MPa amplitude during cyclic deformation<sup>[19]</sup>. Therefore, to identify which kind of dislocation patterns are presented within double twins during the fatigue process, the same fatigued samples at a stress amplitude of 90 MPa were selected for analysis<sup>[19]</sup>.

The microstructures of the fatigued specimens were characterized by optical microscopy (OM), scanning electron microscopy (SEM, Tescan Vega 3 LMH), transmission Kikuchi diffraction (TKD) in the SEM, and transmission electron microscopy (TEM; FEI Tecnai G2 F20). TKD is a novel technique and EBSD (electron backscatter diffraction) was performed on thin foils in transmission mode, which improves the spatial resolution down to 2~5 nm<sup>[20, 21]</sup>. A FEI Helios dual-beam focused ion beam (FIB) was used to prepare the TEM/TKD samples from the fatigued sample. When secondary twins in a primary twin were identified, cross-section samples from the secondary twins regions were extracted for TEM/TKD observation.

## 2 Results and Discussion

### 2.1 Microstructural features on the sample surface

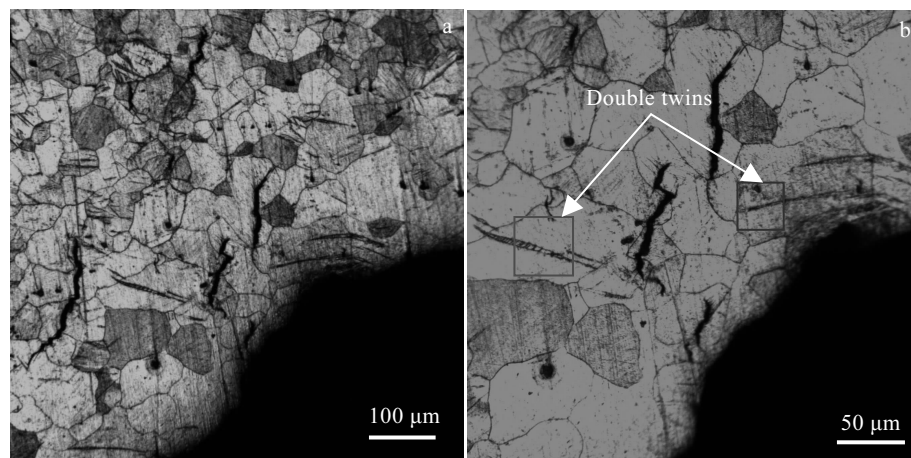


Fig.1 Optical image of the sample surface near the fracture zone (a) and a high-magnification image of double twins (as indicated by red and blue rectangles) (b)

Fig.1 shows the sample surface near the fracture surface of a fatigued sample observed by OM images. As the selected region is slightly away from the fracture surface, it is difficult to observe a large number of twins on the sample surfaces. However, the fatigue process is not just restricted to the final fracture layer, and the observation of the microstructures near the fatigue fracture surface could also provide us with a good understanding of the fatigue mechanism. It is found that some twins are formed near the fracture surface (Fig.1a). High magnification of Fig.1a is present in Fig.1b, showing double twins and some secondary laminas (indicated by red and blue rectangle). This finding is consistent with our previous studies<sup>[19]</sup>. Because the size of TEM sample was rather small, we choose the relatively thinner laminae for TEM observation. The twin lamina indicated by a blue rectangle in Fig.1b was extracted by FIB for TEM/TKD examination.

Fig.2 presents the EBSD inverse pole figure (IPF) map of the TKD sample. Schematic unit cells are inserted to reveal the orientation of the matrix and the tagged twins. As seen in Fig. 2a, primary  $\{10\bar{1}2\}$  twins were observed to be subdivided by secondary  $\{10\bar{1}2\}$  twin boundaries. In addition, the primary  $\{10\bar{1}2\}$  twin boundary consisted of a  $\{10\bar{1}2\}$  twin boundary and  $\{10\bar{1}2\}-\{10\bar{1}2\}$  secondary twin boundaries. Therefore, it can be inferred that these twin laminae were  $\{10\bar{1}2\}-\{10\bar{1}2\}$  secondary twins. Fig. 2b shows the distribution of misorientation angle corresponding to Fig. 2a. The distribution peak around 60° and 86° is related to  $\{10\bar{1}2\}-\{10\bar{1}2\}$  secondary twin boundary and  $\{10\bar{1}2\}$  twin boundary, respectively. These results have confirmed that the secondary twins were  $\{10\bar{1}2\}-\{10\bar{1}2\}$ .

### 2.2 TEM observation

Fig.3 shows a bright-field TEM image of the TKD sample. The electron beam was aligned to  $[11\bar{2}0]$  in Fig.3a. There was a fine twin structure with a thickness of ap-

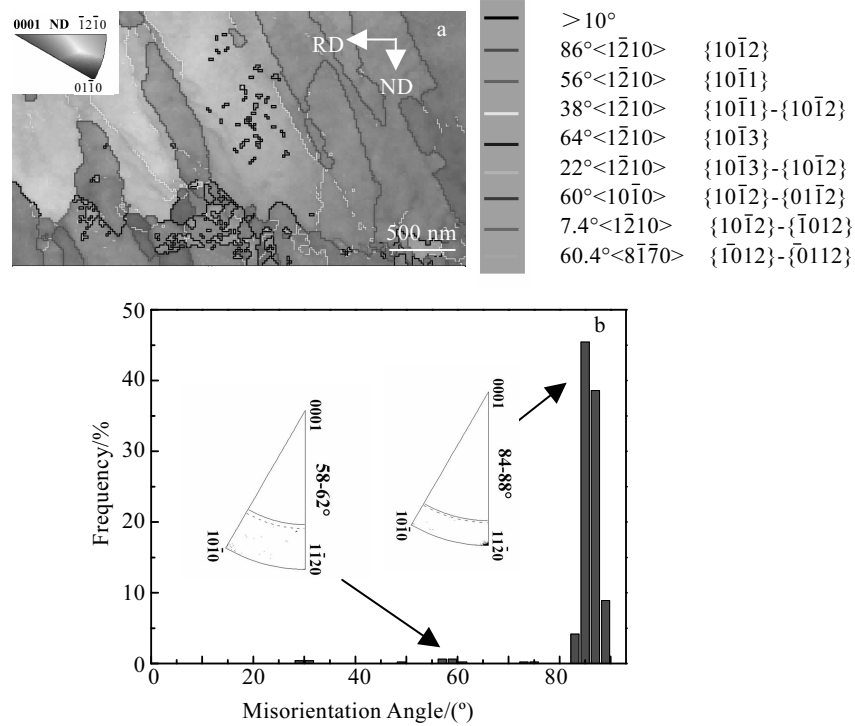


Fig.2 TKD IPF map of the TEM sample extracted by FIB method from Fig.1b (as indicated by blue rectangle) (a) and the distribution of misorientation angles corresponding to Fig.2a (b)

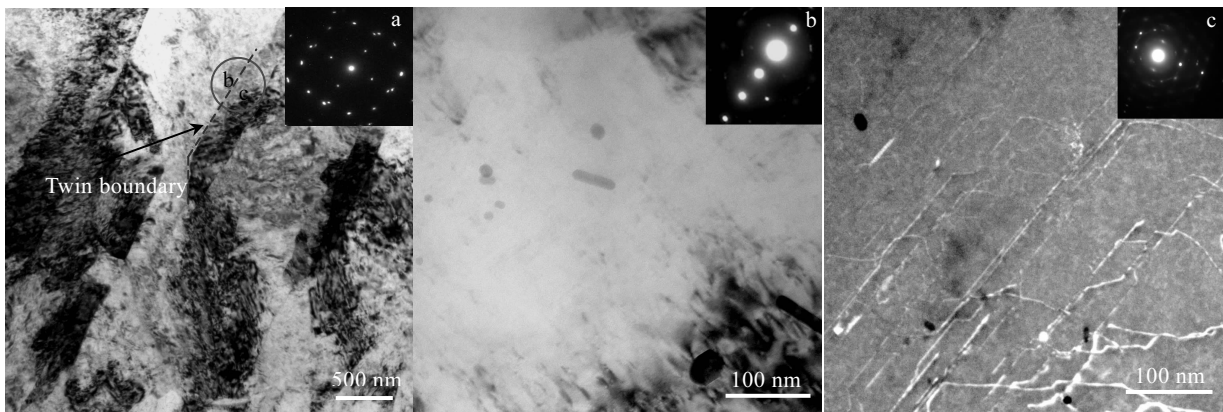


Fig.3 (a) Dislocation structure in the same TKD sample whose stress levels were 90 MPa after high cycle deformation: the electron beam being close to  $\langle 11\bar{2}0 \rangle$ , the inset is the diffraction pattern at the zone axis; (b) TBBF image of region b in Fig.3a, taken using a (0002) reflection close to the  $\langle 10\bar{1}0 \rangle$  zone axis; (c) TBBF image of region c in Fig.3a, taken using a (0002) reflection close to the  $\langle 10\bar{1}0 \rangle$  zone axis

proximately 200 nm, and these twins were parallel to each other. This demonstrates that the twins were the same twin variant<sup>[22]</sup>. The diffraction pattern in the circled area is provided as insets in the micrographs (Fig.3a), which includes a primary twinned region and a secondary twinned region. The pattern indicates that these secondary twins were a  $\{10\bar{1}2\}$  twin type. Other laminae were also identified using

the same method, and all the results indicate that such  $\{10\bar{1}2\}$ - $\{10\bar{1}2\}$  secondary twins widely exists in the fatigued samples.

Dislocations in magnesium and its alloy have been investigated by a number of researchers<sup>[7, 9, 13, 23]</sup>. Magnesium has a hexagonal close-packed (hcp) crystal structure, where the dominant slip mode has a Burgers vector of

$1/3\langle 11\bar{2}0 \rangle$  on the basal plane<sup>[24, 25]</sup>. Such slip mode cannot accommodate strains along the  $c$ -axis. A number of investigators have performed  $c$ -axis compression experiments on single crystals to activate and study non-basal slip<sup>[9, 12, 14]</sup>. The results show that pyramidal slip was activated to accommodate the plastic strain along  $c$ -axis<sup>[15, 26]</sup>. To identify different types of dislocations in hcp materials, i.e.  $\langle a \rangle$ ,  $\langle c \rangle$ , and  $\langle c+a \rangle$ , two-beam bright field (TBBF) TEM techniques were used. The “ $g \cdot b = 0$ ” visibility criteria were used well for identification of dislocations. For example, the Burgers vector of type  $\langle a \rangle$  dislocations is perpendicular to that of  $\langle c \rangle$  dislocations; thus, we can use (0002) and  $(2\bar{1}\bar{1}0)$  reflections to image and differentiate these dislocations. If there are  $\langle c+a \rangle$  dislocations present, they should appear in images of both reflections.

Fig.3b and Fig.3c show the TBBF images under  $g = 0002$  with zone axis  $\langle 01\bar{1}0 \rangle$  of  $\{10\bar{1}2\}$  primary twin region and  $\{10\bar{1}2\}$ - $\{10\bar{1}2\}$  twin region (labeled as ‘b’ and ‘c’, respectively in Fig.3a). In Fig.3b, no dislocations can be seen, according to  $g \cdot b = 0$  criterion, indication that no  $\langle c+a \rangle$  dislocations were present within  $\{10\bar{1}2\}$  primary twin region. While two types  $\langle c+a \rangle$  dislocations were observed in Fig.3b. One type of dislocations was composed of straight line. The straight dislocations were parallel to the basal plane trace, which were confined on the basal plane. The other type of dislocations was tangled and curved. This type of dislocation array has been previously reported as  $\langle c+a \rangle$  dislocations. These observations are in agreement with those previously reported by Geng et al.<sup>[27]</sup> and Obara et al.<sup>[13]</sup>. This configuration was the edge dislocation debris, which was caused by the double cross-slip of  $\langle c+a \rangle$  screw dislocations from the second  $\{11\bar{2}2\}$  pyramidal planes to the first order  $\{10\bar{1}1\}$  pyramidal planes<sup>[27]</sup>. Pyramidal dislocations were found within  $\{10\bar{1}2\}$ - $\{10\bar{1}2\}$  secondary twin laminae.

The formation mechanism of  $\{10\bar{1}2\}$ - $\{10\bar{1}2\}$  secondary twinning was discussed in our recent paper<sup>[14]</sup>.  $\{10\bar{1}2\}$ - $\{10\bar{1}2\}$  secondary twins largely contributed to the local strain accommodation caused by different twin variants. In summary, tension-compression reversed loading led to a complex twinning multiplicity. As reported,  $\{10\bar{1}2\}$  twinning behavior was activated as the first primary twinning mode, and  $\{10\bar{1}2\}$ - $\{10\bar{1}2\}$  and  $\{10\bar{1}2\}$ - $\{10\bar{1}2\}$  secondary twinning occurred within the primary twins. With the  $\{10\bar{1}2\}$  primary twins activating, the  $\{10\bar{1}2\}$  twins were followed by the secondary  $\{10\bar{1}2\}$  twinning evolving within the primary  $\{10\bar{1}2\}$  twins due to its high Schmid factor<sup>[14]</sup>.  $\{10\bar{1}2\}$ - $\{10\bar{1}2\}$  secondary twin laminae were rather thinner within primary twins. We rationalize that plastic relaxation of the stress concentration that occurs within secondary twin zones is limited. Consequently, cracks and voids form in this zone. However, if more plastic deformation modes were available to relieve stress con-

centration, then crack could be hindered. In the current study, pyramidal slip mode was found here to improve the formability facilitating the deformation along  $c$ -axis. Lentz et al.<sup>[18]</sup> reported that pyramidal slip can play a vital role in plastic strain relaxation within secondary twin laminae. The authors<sup>[28-30]</sup> also performed examination on polycrystalline pure Mg and its alloy, and the possible existence of pyramidal dislocations was indeed presented in hcp Mg and its alloy. The present work showed that pyramidal slip was activated inside  $\{10\bar{1}2\}$ - $\{10\bar{1}2\}$  secondary twins region. The interactions between secondary twinning dislocations and primary twinning dislocations tended to reduce the excess energy around the secondary twin boundaries. Therefore, it is suggested that the interactions are driven for accommodation of the stress concentration around secondary twin boundaries. Thus, these interactions of the secondary twinning dislocations with secondary twin boundaries may induce specific stress concentration inside the secondary twin region. In cyclic deformation, many dislocations will be absorbed by tension-compression reversed loading, and piled up around secondary twin boundaries. In such cases, the stress concentration around secondary twin boundaries cannot be sufficiently accommodated by the interaction of primary twin dislocations and secondary twin dislocations. Therefore, pyramidal slips will be activated by large stress concentration caused by increasing loading cycles.

### 3 Conclusions

1) Pyramidal dislocations are observed within  $\{10\bar{1}2\}$ - $\{10\bar{1}2\}$  secondary twins during the cyclic deformation. These findings serve as a guide for further studies in which introduction of  $\langle c+a \rangle$  dislocations is needed, and also provide a quantitative evaluation of pyramidal behavior in hcp metals.

2) The revealed pyramidal slips behavior is expected to play an important role in understanding the complicated slip behavior in hcp Mg.

### References

- 1 Wu W, Lee S Y, Paradowska A M et al. *Materials Science and Engineering A*[J], 2012, 556(9): 278
- 2 Hazeli K, Askari H, Cuadra J et al. *International Journal of Plasticity*[J], 2015, 68: 55
- 3 Dallmeier J, Huber O, Saage H et al. *Materials & Design*[J], 2015, 70: 10
- 4 Azadi M, Farrahi G H, Winter G et al. *Materials & Design*[J], 2014, 53(1): 639
- 5 Duan G S, Wu B L, Du X H et al. *Materials Science and Engineering A*[J], 2014, 603(6): 11
- 6 Koike J, Fujiyama N, Ando D et al. *Scripta Materialia*[J], 2010, 63(7): 747
- 7 Koike J, Kobayashi T, Mukai T et al. *Acta Materialia*[J], 2003, 51(7): 2055

- 8 Koike J, Ohyama R. *Acta Materialia*[J], 2005, 53(7): 1963
- 9 Agnew S R, Horton J A, Yoo M H. *Metallurgical and Materials Transactions A*[J], 2002, 33(3): 851
- 10 Tang Y, El-Awady J A. *Materials Science and Engineering A*[J], 2014, 618: 424
- 11 Tang Y, El-Awady J A. *Acta Materialia*[J], 2014, 71: 319
- 12 Xie K Y, Alam Z, Caffee A et al. *Scripta Materialia*[J], 2016, 112: 75
- 13 Obara T, Yoshinga H, Morozumi S. *Acta Metallurgica*[J], 1973, 21(7): 845
- 14 Syed B, Geng J, Mishra R K et al. *Scripta Materialia*[J], 2012, 67(7-8): 700
- 15 Tan L, Zhang X, Sun Q et al. *Materials Science and Engineering A*[J], 2017, 699: 247
- 16 Weygand D, Gumbsch P. *Materials Science and Engineering A*[J], 2005, 400-401(1): 158
- 17 Xin R L, Ding C H, Guo C F et al. *Materials Science and Engineering A*[J], 2016, 652(116): 42.
- 18 Lentz M, Risse M, Schaefer N et al. *Nature Communications*[J], 2016, 7: 11 068
- 19 Tan L, Zhang X, Xia T et al. *Materials Science and Engineering A*[J], 2018, 711: 205
- 20 Johansson J, Persson C, Lai H et al. *Materials Science and Engineering A*[J], 2016, 662: 363
- 21 Zhu S Q, Yan H G, Liao X Z et al. *Acta Materialia*[J], 2015, 82: 344
- 22 Khosravani A, Fullwood D T, Adams B L et al. *Acta Materialia*[J], 2015, 100: 202
- 23 Yoo M H, Morris J R, Ho K M et al. *Metallurgical and Materials Transactions A*[J], 2002, 33(3): 813
- 24 Yoo M H, Agnew S R, Morris J R et al. *Materials Science and Engineering A*[J], 2001, 319-321(15): 87
- 25 Agnew S R, Tome C N, Brown D W et al. *Scripta Materialia*[J], 2003, 48(8): 1003
- 26 Ando D, Koike J, Sutou Y. *Acta Materialia*[J], 2010, 58(13): 4316
- 27 Geng J, Chisholm M F, Mishra R K et al. *Philosophical Magazine*[J], 2015, 95(35): 3910
- 28 Li B, Yan P F, Sui M L et al. *Acta Materialia*[J], 2010, 58(1): 173
- 29 Ghazisaeidi M, Curtin W A. *Modelling and Simulation in Materials Science and Engineering*[J], 2013, 21(5): 055 007
- 30 Kim K H, Jeon J B, Kim N J et al. *Scripta Materialia*[J], 2015, 108: 104

## 高周疲劳变形中二次孪晶与锥面位错之间的关系

谭力, 张喜燕, 夏挺, 黄光杰, 刘庆  
(重庆大学, 重庆 400044)

**摘要:** 采用金相显微镜(OM), 扫描电镜(SEM), 透射菊池衍射(TKD)和透射电子显微镜(TEM)表征技术, 研究了高周疲劳变形后的 Mg-3Al-1Zn 镁合金的典型断口组织特征, 二次孪晶内部的横切面区域被提取出来进行 TEM 和 TKD 观察。结果显示断口边缘附近的区域有大量的  $\{10\bar{1}2\}$ - $\{10\bar{1}2\}$  二次孪晶, 双束明场技术(TBBF)应用于研究二次孪晶边界的位错类型。研究发现锥面位错在  $\{10\bar{1}2\}$ - $\{10\bar{1}2\}$  二次孪晶内部被大量的激活, 这被认为锥面位错与二次孪晶有关联。二次孪晶内部的局部应力集中将导致锥面位错的形成。

**关键词:** 二次孪晶; 锥面位; 镁合金; 疲劳

---

作者简介: 谭力, 女, 1985年生, 博士, 重庆大学材料科学与工程学院, 重庆 400044, E-mail: 187178457@qq.com